RSC Advances

This is an *Accepted Manuscript*, which has been through the Royal Society of Chemistry peer review process and has been accepted for publication.

Accepted Manuscripts are published online shortly after acceptance, before technical editing, formatting and proof reading. Using this free service, authors can make their results available to the community, in citable form, before we publish the edited article. This *Accepted Manuscript* will be replaced by the edited, formatted and paginated article as soon as this is available.

You can find more information about *Accepted Manuscripts* in the **Information for Authors**.

Star-Shaped Polyphosphoesters with Reactive End Groups Synthesized via Acyclic Diene Metathesis Polymerization and their Transformation to Nanostructures

Liang Ding,[a,*] Jun Wei,[a] Jun Qiu,[a] Jingjing Wang[a] and Zhenshu Zhu[b,c**]

[a] School of Materials Engineering, Yancheng Institute of Technology, Yancheng, 224051, China

[b] Key Laboratory of Drug Quality Control and Pharmacovigilance (China Pharmaceutical University), Ministry of Education, Department of Pharmaceutical Analysis, China Pharmaceutical University, Nanjing 210009, China

[c] Department of Chemical and Biomolecular Engineering, National University of Singapore, 117578, Singapore

*Corresponding authors. Tel.: +86 515 88232258; Fax: +86 515 88298872.

E-mail addresses: dl1984911@ycit.edu.cn (L. Ding), zhuzs@cpu.edu.cn (Z. Zhu).

ABSTRACT: Four-arm star shaped polyphosphoesters are synthesized via acyclic diene metathesis (ADMET) polymerization. This is accomplished by utilizing a phosphoester functional asymmetric α,ω-diene containing a terminal double bond and an acrylate, which is polymerized in the presence of a phosphate compound with multifunctional terminal acrylates as selective and irreversible chain transfer agent using Hoveyda–Grubbs second generation catalyst. High cross-metathesis selectivities hare achieved at low temperatures enabling good control over molecular weights. These reactive star polymers were readily converted, by thiol-Michael addition click reaction of the end groups in dilute solution, to novel thiol-functionalized polymers. Subsequently, hybrid nanostructures are successfully fabricated through covalent integration of Au nanoparticles with this new type of polyphosphoesters, which is shown as one interesting application of such functionalized metathesis polymers.

KEYWORDS: Star-polyphosphoesters; acyclic diene metathesis (ADMET) polymerization; thiol-Michael addition click reaction; hybrid nanostructure

Introduction

The development of synthetic methods leading to well-defined polymers is an essential step towards control over materials properties.[1] Acyclic diene metathesis (ADMET) polymerization is a quantitative reaction tolerating many functional groups, yields only the desired linear polymer, and releases ethylene as an outgrowth.[2] Usually, symmetric α,ω-dienes are employed to obtain polymers with a defined repeat unit structure. This polymerization technique is usually applied to prepare the desired macromolecular architectures.[3] Among these polymer structures, star-shaped polymers in particular have attracted great attention because of their unique physical properties and higher end-group functionality compared with their linear counterparts. Moreover, star-shaped polymers have different rheological and mechanical properties and exhibit higher degrees of end group functionality. Controlled synthesis of star polymers also contributes to the elucidation of structure-property relationships in polymer science.[4] The preparation of star-shaped polymers can be divided into two major synthetic methods: the "arm first" method, where the living linear polymers are linked by adding a cross-linkable monomer, which leads to the formation of a cross-linked core, and the "core first" method, where the controlled polymerization occurs from a multifunctional initiator or precursor molecule.[5] By these methods, the physical properties of the star-shaped polymers can be desirably adjusted by adapting the size, composition and number of the arms, which facilitates their application in materials. Many studies have been published on the synthesis of well-defined star-shaped polymers through different polymerization mechanisms, such as living radical,[5,6] cationic or anionic polymerization,[7] ring opening polymerization,[8] and ring opening metathesis polymerization (ROMP).[9]

Meier recently introduced the concept of a selective head-to-tail ADMET

polymerization using a monomer containing both a terminal double bond and an acrylate. Such monomers polymerize with high cross metathesis selectivity, enabling access to different polymer architectures if a selective and irreversible chain stopper (mono- or multi-functional acrylate) is added.[10] The chain transfer agent allows control over the molecular weight and direct functionalization of the ADMET polymer by selective reaction with only one of the end groups (terminal double bond). Based on this principle, diverse homo- and co-polymers were able to be synthesized.[11]

In recent projects, we have been focusing on the development of novel potentially biodegradable and biocompatible polyphosphoesters (PPEs). PPEs can be degraded by several enzymes such as phosphatases and phosphodiestereases and/or by basic or acidic hydrolysis.[12] In spite of this obvious benefit, PPEs are only scarcely found in recent studies, even if they are easily accessible and allow the feasible synthesis of a great variety of functional materials. The combination of phosphorus chemistry with metathesis allows tailoring of the polymer functionality due to the high functional group tolerance of modern ruthenium metathesis catalysts.[13] Wurm currently presented an expansion of the metathesis polymerization towards PPEs from a step-growth ADMET polymerization[14] to the chain-growth ROMP.[15] Based on these precedents, we reported the synthesis of more complex metathesis PPE architectures, such as AB-alternating, di- and tri-block, cyclic and hyperbranched PPEs via ADMET polymerization.[16] However, functional star-shaped PPEs have not been synthesized and further exploited.

Consequently, building upon our experience with cross metathesis reactions and ADMET polymerization, we wanted to further exploit the cross-metathesis selectivity between terminal olefins and acrylates for the synthesis of defined star-shaped PPEs via ADMET polymerization. Phosphate monomer containing both a terminal olefin

and an acrylate functional group would first polymerize only by head-to-tail additions. Then, the introduction of a phosphate compound containing multifunctional terminal acrylates, as selective chain stopper to this polymerization could result in the formation of star-shaped PPEs. In addition, the acrylate end-groups, which are directly obtained with very high end-group fidelity, could be easily transformed into a new type of the thiol-functionalized PPEs with fixed nanostructures by the thiol–ene reaction, and they have the ability to covalently conjugate Au nanoparticles onto the surface to fabricate hybrid nanostructure (Scheme 1). Because of the covalent linkage between surface thiol groups and Au nanoparticles, this novel type of hybrid nanostructure was highly stable.[17]
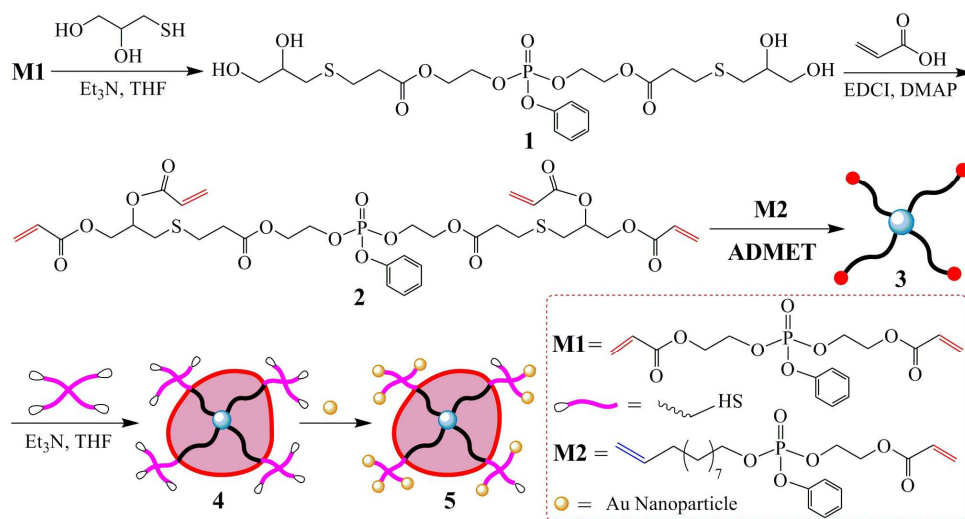
Scheme 1   Illustration for preparation of star-shaped polyphosphoesters via ADMET polymerization and hybrid nanostructures by coupling Au nanoparticles with thiol-functionalized polymers

Experimental section

Materials

Phenyl dichlorophosphate (99%), 2-hydroxyethyl acrylate (>96%), acrylic acid (99%), 1-[3-(dimethylamino)propyl]-3-ethylcarbodiimide hydrochloride (EDCI·HCl, 99%),

3-mercapto-1,2-propanediol (90+%), 4-dimethylaminopyridine (DMAP) (98%), [1,3-bis(2,4,6-trimethylphenyl)-2-imidazolidinylidene]dichloro(*o*-isopropoxyphenylm ethylene)ruthenium (Hoveyda–Grubbs second generation catalyst) (98%), chloroauric acid, 10-undecen-1-ol (98%), pentaerythritol tetra(3-mercaptopropionate) (>85%), and tetrakis(hydroxymethyl)phosphonium chloride (THPC, ca. 80% in water) were purchased from Energy Chemical and used as received without purification. Solvents were distilled over drying agents under nitrogen prior to use. Triethylamine (Et_3N) and pyridine were freshly distilled and dried. Monomers **M1** and **M2** were synthesized as reported previously in our group.[16]

Characterization

^1H (500 MHz) and ^{13}C (125 MHz) NMR spectra were recorded using tetramethylsilane as an internal standard in $CDCl_3$ on a Bruker DPX spectrometer. Phosphoric acid (85%) was used as the external reference for ^{31}P NMR analysis. Relative molecular weights and molecular weight distributions were measured by gel permeation chromatography (GPC) equipped with a Isocratic HPLC pump, a refractive index detector, and a set of Waters Styragel columns (7.8 × 300 mm, 5 μm bead size; 10^3, 10^4, and 10^5 Å pore size). GPC measurements were carried out at 35 °C using THF as the eluent with a flow rate of 1.0 mL/min. The system was calibrated with polystyrene standards. FTIR spectra were recorded on a Nicolet Nexus 670 in the region of 4000–400 cm^{-1} using KBr pellets. UV–vis absorption spectra were measured on an Agilent Cary 60 spectrometer. Gas chromatography (GC) was measured by Agilent 6890 series GC system instrument equipped with a flame ionization detector and a capillary column (HP-5. 0.25 mm × 30 m), using decane as an internal standard. T_{inj} 280 °C, T_{detec} 280 °C, T_{init} 50 °C (10 °C/min), carrier gas: N_2. High-resolution mass spectrometry (HRMS) data were recorded on a Waters GCT

Premier mass spectrometer with electron ionization mode. Elemental analysis (EA) was conducted with an Elementar vario EL. The hydrodynamic diameter was determined by means of dynamic light scattering (DLS) analysis using a Malvern Zetasizer Nano-ZS light scattering apparatus (Malvern Instruments, U.K.) with a He-Ne laser (633 nm, 4 mW). Atom force microscopy (AFM) observations were performed on SPM AJ-III atomic force microscope at a measure rate of 1.0005 Hz in the tapping mode, and the AFM images were obtained at room temperature in air. Transmission electron microscopy (TEM) was performed on a JEM-200CX microscope operating at an acceleration voltage of 200 kV.

Polymerizations were carried out in Schlenk tubes under dry nitrogen atmosphere.

Synthesis of phenyl tetrahydroxylphosphate compound (1)

M1 (3.7 g, 10 mmol), 3-mercapto-1,2-propanediol (5.18 g, 48 mmol), triethylamine (6.06 g, 60 mmol) and CH_2Cl_2 (100 mL) were charged into a 250 mL round-bottom flask equipped with a magnetic stirrer under nitrogen atmosphere, and the mixture was stirred overnight at room temperature. The resulting solution was washed with 1 M HCl, saturated $NaHCO_3$ aq., and water. The organic layer was separated and dried over anhydrous Na_2SO_4, and concentrated to afford a clear liquid **1** (5.32 g, 90.8% yield). ^{1}H NMR ($CDCl_3$), δ (ppm): 7.36–7.12 (m, 5H, Ar*H*), 4.43–4.37 (m, 4H, CH_2CH_2OCO), 3.80–3.73 (m, 4H, C*H$_2$*CH$_2$OCO), 3.71–3.66 (m, 2H, CH$_2$C*H*CH$_2$), 3.63–3.51 (m, 4H, C*H$_2$*OH), 2.82–2.77 (m, 4H, SC*H$_2$*CH$_2$OCO), 2.73–2.61 (m, 8H, SCH_2CH_2OCO + SCH$_2$C*H$_2$*OCO). ^{13}C NMR ($CDCl_3$), δ (ppm): 172.11, 152.26, 131.46, 121.98, 120.27, 71.15, 66.52, 65.57, 64.21, 36.69, 35.80, 29.23. ^{31}P NMR, δ (ppm): −2.86. GC: single peak was observed. EI/HRMS: Calcd. for $C_{22}H_{35}O_{12}S_2P$: 586.6178; found: 586.6165. Anal. calcd for C: 45.05, H: 5.97, O: 32.76, S: 10.92; Found C: 45.07, H: 5.95, O: 32.78, S: 10.93.

Synthesis of phenyl tetraacryloyloxyphosphate compound (2)

Acrylic acid (3.46 g, 48 mmol), compound **1** (4.69 g, 8 mmol), and DMAP (0.48 g, 3.84 mmol) were dissolved in CH_2Cl_2 (60 mL), and the mixture was stirred at 0 ºC for 15 min. EDCI (9.2 g, 48 mmol) was then added to the former solution, and stirred for 3 days under nitrogen flow after the solution warmed to room temperature. The resulting solution was washed three times with deionized water (3 × 80 mL), and the organic layer was dried over anhydrous Na_2SO_4. Solvent was then evaporated and the crude product was purified by silica gel chromatography eluted with methylene chloride/petroleum ether (15/1) to give a colorless liquid **2** (4.89 g, 76.2% yield). ^{1}H NMR ($CDCl_3$), δ (ppm): 7.37–7.14 (m, 5H, Ar*H*), 6.36–6.27 (d, 4H, OCOCH=C*H*), 6.20–6.12 (m, 4H, OCOC*H*=CH), 5.98–5.91 (m, 4H, OCOCH=C*H*), 4.81–4.76 (m, 2H, CH₂C*H*CH₂), 4.42–4.23 (m, 8H, CH₂=CHOCOC*H*₂ + OCOC*H*₂CH₂), 3.91–3.78 (m, 4H, OCOCH₂C*H*₂), 2.85–2.77 (m, 2H, CH₂SC*H*₂CH₂), 2.69–2.50 (m, 8H, C*H*₂SCH₂CH₂ + CH₂SCH₂C*H*₂). ^{13}C NMR ($CDCl_3$), δ (ppm): 171.92, 165.36, 151.97, 131.58, 130.81, 127.98, 122.15, 120.79, 77.42, 67.30, 64.16, 36.24, 33.67, 28.29. ^{31}P NMR, δ (ppm): −3.12. GC: single peak was observed. EI/HRMS: Calcd. for $C_{34}H_{43}O_{16}S_2P$: 802.8117; found: 802.8145. Anal. calcd for C: 50.87, H: 5.36, O: 31.92, S: 7.98; Found C: 50.88, H: 5.34, O: 31.90, S: 8.01.

Synthesis of star-shaped polyphosphoesters (3) from M2 and compound 2 as core

In a nitrogen-filled Schlenk tube, monomer **M2** and the desired amount of selective chain stopper (**2**) were degassed by three freeze-vacuum-thaw cycles. The mixture was heated to 40 °C while stirring and then a solution of Hoveyda–Grubbs second generation catalyst (0.5 mol% to monomer) in 0.5 mL of $CHCl_3$ degassed with the same procedure was added. After the reaction mixture was stirred for 24 h, the polymerization was quenched by adding THF (2 mL) and ethyl vinyl ether with

stirring for 30 min. The solution was precipitated into an excess of methanol, and the precipitate was isolated by filtration, dried under vacuum for 24 h to give the star-shaped PPEs. ^{1}H NMR (CDCl$_3$), δ (ppm): 7.39–7.21 (m, ArH), 7.02–6.95 (m, OCOCH=CH), 5.99–5.87 (d, OCOCH=CH), 4.90–4.78 (m, CH$_2$CHCH$_2$), 4.51–4.19 (m, CH$_2$=CHOCOCH_2 + OCOCH_2CH$_2$), 4.04–3.72 (m, OCOCH$_2$CH_2), 2.83–2.76 (m, CH$_2$SCH_2CH$_2$), 2.67–2.52 (m, CH_2SCH$_2$CH$_2$ + CH$_2$SCH$_2$CH_2), 2.12–1.77 (m, OCOCH=CHCH_2), 1.62–1.47, 1.45–0.92 (m, (CH_2)$_7$).

Transformation of end group functionalization of star-shaped polyphosphoesters to the thiol-functionalized polymer (4)

Star-shaped PPEs **3** (90 mg, 0.005 mmol, $M_{n,NMR}$ = 17900) and pentaerythritol tetra(3-mercaptopropionate) (49 mg, 0.1 mmol) (1: 5 molar ratio) were dissolved in dried THF (100 mL, C = 5 × 10^{-6} mol/L) at room temperature under N$_2$ atmosphere. 1-Dodecylamine (9 mg, 10 wt%) was added as a catalyst and the mixture was stirred for 2 h. The solution was concentrated under vacuum and precipitated into an excess of methanol, and the precipitate was isolated to give a thiol-functionalized polymer **4**. ^{1}H NMR (CDCl$_3$), δ (ppm): 7.37–7.22 (m, ArH), 7.01–6.92 (m, OCOCH=CH), 5.89–5.79 (d, OCOCH=CH), 4.96–4.77 (m, CH$_2$CHCH$_2$), 4.63–4.37 (m, CH$_2$=CHOCOCH_2 + OCOCH_2CH$_2$), 3.82–3.69 (m, OCOCH$_2$CH_2 + CCH_2OCO), 2.78–2.26 (m, CH$_2$SCH_2CH$_2$ + CH_2SCH$_2$CH$_2$ + CH$_2$SCH$_2$CH_2 + CH_2SH), 2.02–1.81 (m, OCOCH=CHCH_2), 1.68–1.27, 1.25–0.91 (m, CH$_2$SH + (CH_2)$_7$).

Synthesis of Au nanoparticles

Au nanoparticles were prepared by the Duff method.[18] 1.0 M NaOH (3.0 mL) and THPC solution (2.0 mL), which had been prepared by mixing THPC solution (24 μL, 80%) with water (2.0 mL), were added into deionized water (91.0 mL). The mixture was vigorously stirred for 5 min, followed by the rapid addition HAuCl$_4$ aqueous

solution (4.0 mL, 1 wt%), the color of the solution changed to dark brown immediately. After the reaction mixture was stirred for another 2 h, the solution was concentrated under vacuum, filtered through an Isopore polycarbonate filter membrane of 0.2 μm nominal pore size, and then stored at 4 °C prior to further use.

Conjugation of Au nanoparticles onto thiol-functionalized polyphosphoesters

A solution of the thiol-functionalized PPEs **4** in THF (2 mL) at a concentration of 0.5 mg/mL and the aqueous solution of Au NPs (about 5 mL) were mixed with vigorous stirring for 4 h in the dark at room temperature, leading to the attachment of Au nanoparticles on the thiol groups of PPEs **4**. To remove the remaining free Au nanoparticles, the above solution was centrifuged. After decanting the supernatant, the precipitate was washed with deionized water for 4 times, and then collected the product to be dried for 3 days.

Results and Discussion

Multifunctional acrylate selective chain stopper

As already mentioned, the approach to the synthesis of star-shaped polymers via ADMET polymerization involves the reaction of a multifunctional acrylate with an unsymmetric α,ω-diene containing both a terminal double bond and an acrylate. The reaction will thus proceed by head-to-tail ADMET polymerization. A similar approach was used by Meier et al. for the synthesis of star-shaped (block) copolymers, in which polymerization was terminated with multifunctional (tri-, and tetra-) acrylates.[10,11c] We chose phenyl tetraacryloyloxyphosphate compound (**2**), which was successfully prepared by a two-step technique, as a core molecule and irreversible and selective chain stopper to obtain four arm star-shaped polyphosphoesters. As the first step, the prepared α,ω-diacrylate phosphate, **M1**, contained two acrylate groups, which could allow for the direct reaction with 3-mercapto-1,2-propanediol in the

presence of triethylamine by thiol–Michael addition click reaction. Then, **2** was synthesized from an esterification reaction of the obtained phenyl tetrahydroxylphosphate compound **1** with acrylic acid catalyzed by DMAP in CH₂Cl₂ at room temperature (Scheme 1). The structure and purity of compound **1** and **2** were fully tested by GC–MS, elemental analysis, FTIR and NMR spectroscopy, which affirmed the successful preparation of resulting compounds with the expected chemical structure.
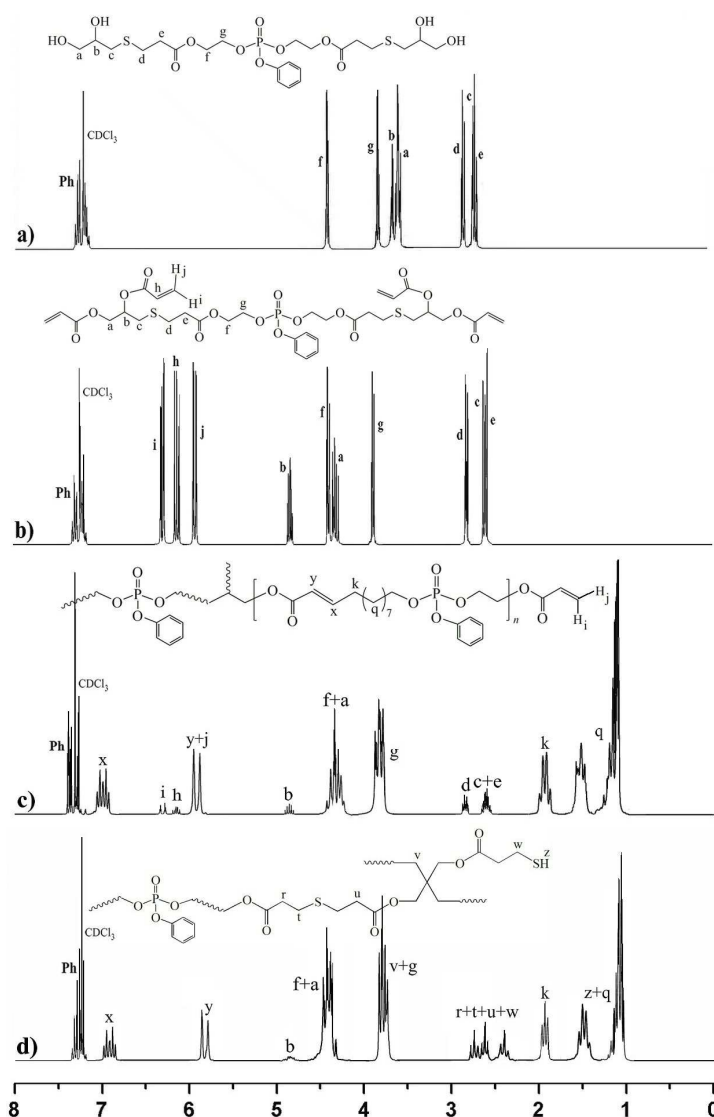
Fig. 1　¹H NMR spectra for (a) tetrahydroxylphosphate compound **1**, (b) tetraacryloyloxyphosphate chain stopper **2**, (c) star-shaped polyphosphoester **3**, and (d)

thiol-functionalized polyphosphoester **4**

Star-shaped polyphosphoesters via ADMET polymerization

We have investigated and established the ADMET polymerization conditions of monomer **M2**, and achieved a high terminal olefin-to-acrylate metathesis selectivity of 98% (calculated by ^{1}H NMR) when using 0.5 mol% of Hoveyda–Grubbs second generation catalyst at 40 °C.[16c] Herein, monomer **M2** was reacted with chain stopper **2** in the presence of 2 mol% (to total acrylate groups) of Hoveyda–Grubbs second generation catalyst. For the selective chain stopper, the monomer/chain stopper molar ratio was precisely adjusted (20: 1–40: 1) to obtain star-shaped PPEs with different length of monomers per arm. Under this reaction conditions, self-metathesis of these end-groups will be negligible and crosslinking is therefore avoided. Indeed, the analysis of the resulting product by ^{1}H NMR (Fig. 1c) showed new formed internal α,β-unsaturated ester functions at 6.99 (x) and 5.82 ppm (y), and the internal olefin peak of the unsaturated polyolefin at 5.38 ppm was not observed, indicating that ADMET polymerization between terminal olefins almost did not happen. Additionally, the average degree of polymerization (DP) and the molecular weight are calculated from the end-group analysis of the ^{1}H NMR spectrum. DP is estimated by the integral intensity ratio of newly formed internal acrylate protons on each arm at 6.99 ppm to that of terminal acrylate protons on polymer chain at 6.36 ppm as follows: DP = $4 \times n = 4S_x/S_i$, and then used to determine the number-average molecular weight of star-shaped PPEs **3**, $M_{n,NMR} = DP \times M_{(M2)} + M_{(2)} - 4 \times M_{(ethylene)}$. It is delighted to note DPs close to the expected ones (Table 1) and a good correlation between core, backbone and end group signals.

Table 1 Analytical data of star-shaped polyphosphoesters via ADMET polymerization with selective chain stopper

Polymer	Yield[a] (%)	[M]/[CS]	$M_{n,GPC}$[b]	M_w/M_n[b]	DP[c]	$M_{n,NMR}$[d]
3a	89	20: 1	13500	1.71	21.6	9800
3b	88	30: 1	18700	1.76	33.9	15100
3c	91	40: 1	24600	1.68	40.7	17900
4c	96	–	21800	1.62	–	–

[a] Obtained gravimetrically from the dried polymer.

[b] Determined by gel permeation chromatography in THF relative to monodispersed polystyrene standards.

[c] DP = $4 \times n$ was obtained by ^{1}H NMR spectroscopy, where $n = S_x/S_i$.

[d] $M_{n,NMR} = DP \times M_{(M2)} + M_{(2)} - 4 \times M_{(ethylene)}$, where $M_{(M2)} = 424$, $M_{(2)} = 802$, and $M_{(ethylene)} = 28$.

GPC curves of the star-shaped PPEs (Fig. 2) displayed that **3** had a moderate molecular weight of 13500–24600 with reasonable molecular weight distribution of 1.68–1.76. The molecular weights obtained from GPC curves correlate with the polymerization degrees calculated from the ^{1}H NMR spectra (Table 1), confirming that star-shaped PPEs can be synthesized via olefin metathesis in the presence of a low catalyst loading and at low temperature, thereby making it possible to tune their molecular weight by adjusting the monomer/core ratio. It must be pointed out that the ongoing ADMET chemistry is certainly a mixture of step-growth chemistry of **M2** (homo-oligomerization) and simultaneous chain-growth of **M2** to the formed star-shaped polymer. Therefore, in the experiments, monomer and catalyst were added in several steps, and the addition of a new batch of catalyst (0.5 mol% to **M2**) in each step was found necessary to observe metathesis activity. More importantly, the formation of free oligomeric species was not observed indicating that the monomer was fully incorporated into the star-shaped polymer.
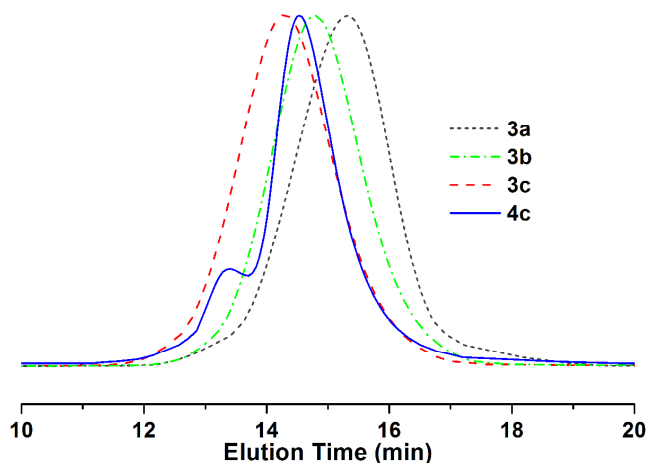
Fig. 2 GPC traces of star-shaped polyphosphoesters **3** and thiol-functionalized polyphosphoester **4c**

Thiol-functionalized polyphosphoesters from reactive star-shaped polymers

It is well known that macromolecules with pendant or peripheral acrylate functionalities can be crosslinked in concentrated solution using a variety of chemical transformations to generate covalent links between different chains leading ultimately to a three dimensional network. However, when these crosslinking reactions are performed in ultradilute solution, the covalent links are exclusively formed between segments of the same polymer chain leading to an unimolecular particle.[19] In this article, the peripheral acrylate functionalized star-shaped PPEs are known to react rapidly with thiols by the thiol–ene reaction, and can be converted into other architectures and functionalities.[16a,17,20] Upon addition of the catalyst triethylamine to a mixture of a tetrathiol and star-shaped PPEs bearing terminal acrylates, the thiol-functionalized polymers **4** in Scheme 1 with controlled size and morphology was formed by means of a thiol-Michael addition click reaction within a short time. Since the ratio of inter- and intra-molecular reactions depends on the concentration of the polymer and reaction time. Usually, at low concentration of 10^{-5} mol/L, the soluble polymers would be obtained. Prolonging the reaction time or increasing the polymer

concentrations gradually resulted in the appearance of the shoulders at high molecular weight fraction (Figure 3), caused by intermolecular reaction, whereas an insoluble gel was produced from reaction at concentrations above 10^{-3} mol/L (Table 2). A reduction of the concentration to an even lower value would finally lead to a pure product. Therefore, the highly dilute solution of PPEs at 5×10^{-6} mol/L with a short reaction time of 2 h was examined to avoid the intermolecular crosslinking. The resulting products were then analyzed by ^{1}H NMR spectroscopy to determine the conversion and by GPC curve to detect the possible presence of coupled star-shaped PPEs. As depicted in Fig. 1d, the almost complete disappearance of the end acrylate signals (*i*, *h*) and the new peaks of methylene protons (*r*, *t*, *u* and *w*) appeared demonstrated near quantitative conversion. The reduction of the hydrodynamic volume of the obtained polymer **4c**, in comparison to the star polymer **3c**, is illustrated in the GPC curves presented in Fig. 2, which may result from possible intramolecular crosslinking or changing coiling dynamics from peripheral decoration of polymers with tetrathiols.[6c,19]
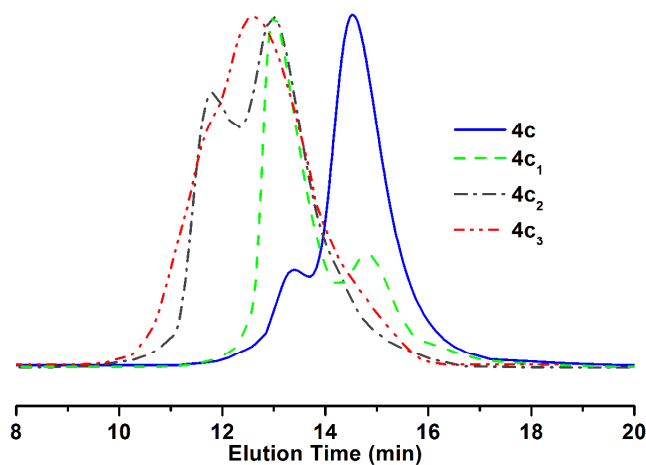

Fig. 3   GPC traces of the thiol-functionalized polyphosphoesters **4c** with different reaction conditions.

Table 2 Reaction conditions and results of the thiol-functionalized polyphosphoesters

4c by means of a thiol-Michael addition click reaction [a]

nanoparticles	time (h)	yield (%)[b]	concentration (mol/L)	$M_{n, GPC}$[c]	PDI[c]
4c	2	96	5×10^{-6}	21800	1.62
4c$_1$	4	95	5×10^{-6}	30500	1.69
4c$_2$	6	97	5×10^{-6}	46900	1.77
4c$_3$	2	91	5×10^{-4}	49700	1.82
4c$_4$	1	99	5×10^{-2}	gel	−

[a] Reactions were run at room temperature for $1 - 6$ h with different concentrations.

[b] Obtained gravimetrically from the dried polymer.

[c] Number-average molecular weight (M_n) and polydispersed index (PDI) were determined by gel permeation chromatography in THF relative to monodispersed polystyrene standards.

To measure the hydrodynamic diameter and polydispersity index (PDI) of the thiol-functionalized polymers **4c**, a portion (1 mL) of the THF solution was taken out from the original reaction mixture and analyzed by DLS. Fig. 4a shows the size and distribution of PPE **4c**, giving the average hydrodynamic diameter of 24 nm and a PDI of 0.191 with a monomodal size-distribution. When **4c** in THF was precipitated from methanol, dried under vacuum, and then redissolved in THF or CHCl$_3$, nanoparticles almost retained the size (28 nm) and distribution (PDI = 0.201). These results indicated that the nanostructure of polymer **4c** were actually stable and reproducible in organic solvents. The morphology of **4c** was examined by AFM. One drop of the dilute solution at concentration of 0.005 mg/mL in THF was spin-coated on the freshly cleaved mica at spinning speed of 1600 rpm for 30 s. The AFM image of individual polymer was given in Fig. 4b, which exhibited a spherical morphology in comparatively uniform size with an average diameter of 20 nm. Further evidence for the formation of spherical morphology was obtained by TEM analysis. The

sample was prepared by dropping the copolymer solution with concentration of 0.005 mg/mL in THF onto the carbon-coated copper grid, followed by air-drying. As a typical TEM image, it can be seen in Fig. 4c that **4c** takes an approximately spherical shape, and well particle dispersion with no aggregated structures. Most of nanoparticles have an average diameter of 16 nm, which is coincident with the DLS result considering the sample in dry state. Although it is hard to evaluate the theoretical diameter for individual star-shaped PPE molecules, it is reasonable to consider these spherical objects from star-shaped PPEs with a number-average molecular weight of 24600, leading to the formation of smaller sized than hyperbranched PPEs, possibly due to the significantly decreased hydrodynamic volume, the existence of chain entanglement, and some random coiling of arms for star-shaped polymer, resulting in a reduced size.[6c,19]
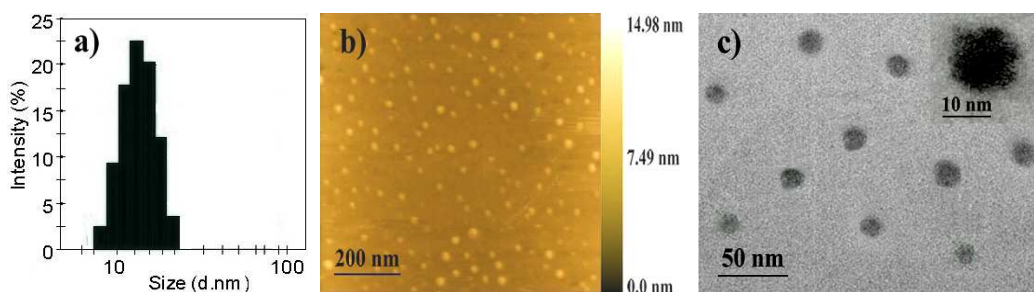

Fig. 4 Thiol-functionalized polyphosphoester **4c** formed by thiol-Michael addition click reaction (a) size and distribution determined by means of DLS in THF, (b) AFM image with concentration of 0.005 mg/mL, and (c) TEM image at 0.005 mg/mL.

Fabrication and characterization of hybrid nanostructure

The significant function of thiol group, which is to form sulfur bonds to metal surfaces, has been exploited largely in materials science and for analytical purposes. Also, such thiol bonding materials play an important role in surface plasmon resonance spectroscopy (SPR).[23] The peripheral thiol groups on the surface of polymers **4** are known to couple rapidly with Au nanoparticles through the covalent

approach.[17,24] To further demonstrate the application of these controlled surface structures, adding the as-synthesized Au nanoparticles with an average diameter of 4 nm (Fig. 6a) into the thiol-functionalized PPEs solution dropwise. A heterogeneous reaction took place that formed polymer/Au hybrid nanostructures.
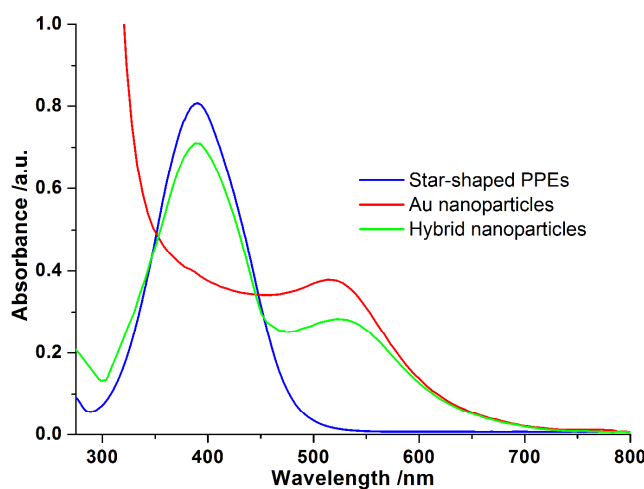

Fig. 5   UV–vis absorption spectra of star-shaped polyphosphoesters, the as-prepared Au nanoparticles, and polymer/Au nanohybrid.

The corresponding UV–vis absorption spectra of nanohybrid in THF (Fig. 5) exhibited a small but discernible SPR peak shift (maximum at 527 nm) comparing to the original Au nanoparticle solution (maximum at 521 nm), indicating that the conjugation of Au nanoparticles onto the thiol-functionalized PPEs surface has increased the local concentration of Au nanoparticles at the sphere surface and decreased the average spatial distance between Au nanoparticles compared with that in the original Au nanoparticles solutions. This may be due to the interparticle interactions of Au nanoparticles on the polymer surface, as well as the lowering of energy states of the Au nanoparticles likely due to their interaction with the functionality of polymers.[25]
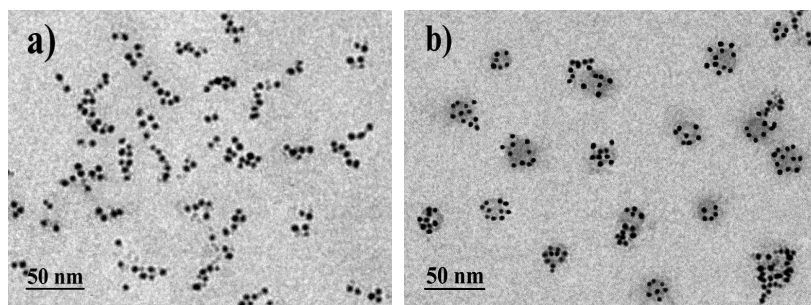
Fig. 6   TEM images of (a) Au nanoparticles and (b) polymer/Au nanohybrid.

Further evidence for the formation of nanohybrid was obtained by TEM analysis. TEM image in Fig. 6b illustrated that nanohybrid **5** was composed of organic polymer **4** and inorganic Au nanoparticles, and displayed a relatively uniform separation as a spherical morphology with an average particle diameter of 18 nm. The Au nanoparticles were individually localized on the surface of the thiol-functionalized PPE spheres and did not show any noticeable aggregation. Since the polymer had much lower electron density than Au nanoparticles, insufficient to be observed by TEM, the polymer backbone appeared as a gray background in polymer/Au nanohybrid.
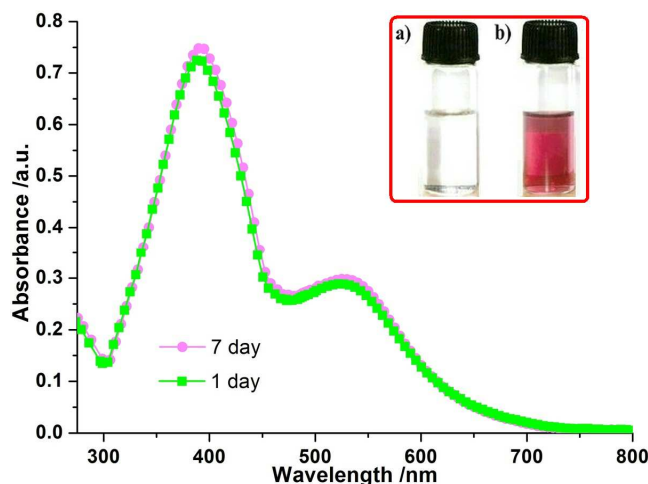

Fig. 7   UV–vis absorption spectra of polymer/Au nanohybrid under different storage time. The insets are the photographs of the as-prepared Au nanoparticles suspension and polymer/Au nanohybrid for different storage times.

Besides, the stabilization of the as-obtained nanohybrid **5** was investigated simply. The initial hydrophilic Au nanoparticles were poorly stable over time. Coating Au nanoparticles on the thiol-functionalized PPE dramatically enhanced their stability, nearly no evolution of the UV–vis spectrum was observed at room temperature for extended storage times of up to 7 days (Fig. 7). It should be noted that the UV–vis absorption spectrum did not show any noticeable aggregation between the conjugated Au nanoparticles, suggesting that surface attached neighboring Au nanoparticles did not come in contact with each other even after being stored for a long time. The insets in Fig. 7 displayed the photographs of Au nanoparticles suspension and polymer/Au nanohybrid, which further affirmed the stabilization of nanohybrid. Au nanoparticles were precipitated after 3 days, and turned their color from pink-red to colorless. After being covalently attached to the surface of the thiol-functionalized PPE, the color of nanohybrid was finally changed to violet in one week. This good stabilization of the as-obtained nanohybrids will be favorable for their applications, such as in catalysis of organic compounds as a colloidal but recyclable catalyst.[17]

Conclusion

We have shown that complex, defined star-shaped polymeric structures can be synthesized via ADMET polymerization of an unsymmetric diene in the presence of suitable multifunctional chain transfer agent. In this work, it has been demonstrated that four-arm star-shaped PPEs were prepared in a controlled way using a phosphoester functional α,ω-diene monomer and small tetraacrylates chain stopper. The molecular weight of these polymers can be well controlled using this polycondensation approach through the monomer/chain transfer agent feed ratio. The reactive star PPEs were converted into a new type of PPEs with comparatively uniform size by means of a thiol-Michael addition click reaction utilizing the

functional tetrathiol. It is also worth mentioning that these thiol-functionalized PPEs enable as a template for the covalent attachment of Au nanoparticles at their surface, hybrid nanostructures were readily obtained with high stability. It is easy to envision that these hybrid nanostructures could lead to a number of applications including catalysis, optical and electronic devices, and sensors.[26] Therefore, the extension of this work is currently underway.

Acknowledgments

References

1 J. M. Frechet, *Science*, 1994, **263**, 1710–1715.

2 J. E. Schwendeman, A. C. Church and K. B. Wagener, *Adv. Synth. Catal.,* 2002, **344**, 597–613.

3 A. H. E. Muller and K. Matyjaszewski, *Controlled and living polymerizations: From mechanisms to applications,* Weinheim, Willey–VCH, 2009.

4 K. Inoue, *Prog. Polym. Sci.,* 2000, **25**, 453–571.

5 a) M. Lammens, D. Fournier, M. W. M. Fijten, R. Hoogenboom and F. Du Prez, *Macromol. Rapid Commun.,* 2009, **30**, 2049–2055; b) N. Ghasdian, E. Church, A. P. Cottam, K. Hornsby, M. Y. Leung and T. K. Georgiou, *RSC Adv.*, 2013, **3**, 19070–19080.

6 a) G. Hart-Smith, H. Chaffey-Millar and C. Barner-Kowollik, *Macromolecules,* 2008, **4**, 3023–3041; b) D. Kul, L. M. Van Renterghem, M. A. R. Meier, S. Strandman, H. Tenhu, S. S. Yilmaz, U. S. Schubert and F. E. Du Prez, *J. Polym. Sci.,*

Part A: Polym. Chem., 2008, **46**, 650–660; c) L. M. V. Renterghem, M. Lammens, B. Dervaux, P. Viville, R. Lazzaroni and F. E. Du Prez, *J. Am. Chem. Soc.,* 2008, **130**, 10802–10811; d) H. Gao and K. Matyjaszewski, *Prog. Polym. Sci.,* 2009, **34**, 317–350.

7 a) H. Shohi, M. Sawamoto and T. Higashimura, *Macromolecules,* 1991, **24**, 2309–2313; b) R. P. Quirk and Y. Tsai, *Macromolecules,* 1998, **31**, 8016–8025; c) R. Matmour, A. Lebreton, C. Tsitsilianis, I. Kallitsis, V. Heroguez and Y. Gnanou, *Angew. Chem. Int. Ed.* 2005, **44**, 284–287; d) T. Shibata, S. Kanaoka and S. Aoshima, *J. Am. Chem. Soc.,* 2006, **128**, 7497–7504.

8 a) J. Y. Chang, H. J. Ji, M. J. Han, S. B. Rhee, S. Cheong and M. Yoon, *Macromolecules,* 1994, **27**, 1376–1380; b) M. A. R. Meier, J.-F. Gohy, C.-A. Fustin and U. S. Schubert, *J. Am. Chem. Soc.,* 2004, **126**, 11517–11521.

9 a) S. Gatard, S. Nlate, E. Cloutet, G. Bravic, J.-C. Blais and D. Astruc, *Angew. Chem. Int. Ed.,* 2003, **42**, 452–456; b) J. W. Liu, J. X. Li, M. R. Xie, L. Ding, D. Yang and L. Y. Zhang, *Polymer,* 2009, **50**, 5228–5235.

10 L. M. D. Espinosa and M. A. R. Meier, *Chem. Commun.,* 2011, **47**, 1908–1910.

11 a) A. Rybak and M. A. R. Meier, *ChemSusChem,* 2008, **1**, 542–547; b) M. Winkler, J. O. Mueller, K. K. Oehlenschlaeger, L. M. D. Espinosa, M. A. R. Meier and C. B. Kowollik, *Macromolecules,* 2012, **45**, 5012–5019; c) L. M. D. Espinosa, M. Winkler and M. A. R. Meier, *Macromol. Rapid Commun.,* 2013, **34**, 1381−1386.

12 S. W. Huang and R. X. Zhuo, *Phosphorus, Sulfur, and Silicon and the Related Elements*, 2008, **183**, 340.

13 C. W. Bielawski and R. H. Grubbs, *Prog. Polym. Sci.,* 2007, **32**, 1−29.

14 F. Marsico, M. Wagner, K. Landfester and F. R. Wurm, *Macromolecules,* 2012, **45**, 8511−8518.

15 T. Steinbach, E. M. Alexandrinob and F. R. Wurm, *Polym. Chem.,* 2013, **4**, 3800−3806.

16 a) L. Ding, J. Qiu, R. Lu, X. Q. Zheng and J. An, *J. Polym. Sci. Part A: Polym. Chem.,* 2013, **51**, 4331−4340; b) L. Ding, R. Lu, J. An, X. Q. Zheng, J. Qiu, *React. Funct. Polym.,* 2013, **73**, 1242−1248; c) L. Ding, X. Q. Zheng, J. An, J. Qiu and R. Lu, *J. Polym. Res.,* 2013, **20**, 287, 1−8.

17 M. R. Xie, L. Ding, Z. W. You, D. Y. Gao, G. D. Yang and H. J. Han, *J. Mater. Chem.,* 2012, **22**, 14108−14118.

18 a) D. G. Duff, A. Baiker and P. P. Edwards, *Langmuir,* 1993, **9**, 2301−2309; b) D. G. Duff and A. Baiker, *Langmuir,* 1993, **9**, 2310−2317; c) C. C. Huang, C. T. Chen, Y. C. Shiang, Z. H. Lin and H. T. Chang, *Anal. Chem.,* 2009, **81**, 875−882.

19 a) D. Mecerreyes, V. Lee, C. J. Hawker, J. L. Hedrick, A. Wursch, W. Volksen, T. Magbitang, E. Huang and R. D. Miller, *Adv. Mater.,* 2001, **13**, 204−208; b) E. Harth, B. V. Horn, V. Y. Lee, D. S. Germack, C. P. Gonzales, R. D. Miller and C. J. Hawker, *J. Am. Chem. Soc.,* 2002, **124**, 8653−8660.

20 a) C. E. Hoyle, and C. N. Bowman, *Angew. Chem. Int. Ed.,* 2010, **49**, 1540−1573; b) X. F. Sui, L. Ingen, M. A. Hempenius and G. J. Vancso, *Macromol. Rapid Commun.,* 2010, **31**, 2059−2063; c) L. Ding, G. D. Yang, M. R. Xie, D. Y. Gao, J. H. Yu and Y. Q. Zhang, *Polymer,* 2012, **53**, 333−341.

21 S. S. Sheiko and M. Moller, *Chem. Rev.,* 2001, **101**, 4099–4123.

22 K. Huang and J. Rzayev, *J. Am. Chem. Soc.,* 2009, **131**, 6880–6885.

23 a) S. R. Johnson, S. D. Evans and R. Brydson, *Langmuir,* 1998, **14**, 6639−6647; b) M. Kuang, D. Y. Wang and H. Mohwald, *Adv. Funct. Mater.,* 2005, **15**, 1611−1616; c) L. Ding, J. Qiu and Z. S. Zhu, *Macromol. Rapid Commun.,* 2013, **34**, 1635−1641.

24 a) H. Xu, J. Xu, X. Jiang, Z. Zhu, J. Rao, J. Yin, T. Wu, H. Liu and S. Y. Liu,

Chem. Mater., 2007, **19**, 2489−2494; b) S. Hilf and A. F. M. Kilbinger, *Macromolecules,* 2009, **42**, 4127−4133; c) J. Y. Mao, X. X. Qi, X. Q. Cao, J. M. Lu, Q. F. Xu and H. W. Gu, *Chem. Commun.,* 2011, **47**, 4228−4230.

25 T. Wang, X. Hu, X. Qu and S. Dong, *J. Phys. Chem. B,* 2006, **110**, 6631−6636.

26 a) G. Wang and W. Sun, *J. Phys. Chem. B,* 2006, **110**, 20901−20905; b) E. C. Cho, S. W. Choi, P. H. C. Camargo, Y. N. Xia, *Langmuir,* 2010, **26**, 10005−10012; c) Y. N. Li, D. S. Yu, L. M. Dai, A. Urbas and Q. Li, *Langmuir,* 2011, **27**, 98–103; d) W. J. Liu, D. R. Sun, J. L. Fu, R. S. Yuan and Z. H. Li, *RSC Adv.***,** 2014, **4**, 11003–11011.

For Table of Contents use only